



NUMERICAL SIMULATION OF AERODYNAMIC PERFORMANCE OF WING WITH SPLIT WINGLETS

MILICA MILIC¹

University of Belgrade, Faculty of Mechanical Engineering Kraljice Marije 16, 11120 Belgrade 35,
mmilic@mas.bg.ac.rs,

JELENA SVORCAN², NEMANJA ZORIC²

University of Belgrade, Faculty of Mechanical Engineering, Kraljice Marije 16, 11120 Belgrade 35,
jsvorcan@mas.bg.ac.rs, nzoric@mas.bg.ac.rs,

Abstract: Winglet is an additional surface in a form of vertical or horizontal extension of the wing. The shape of winglet changed during the development period and depending on the type of aircraft on which they were installed. Due to its benefits and influence on aircraft performance during the flight, the standard end of wing has been replaced by new configurations. The geometry of the winglet depends on the required performance and is unique in each application. The angle (or edge) of the winglet, its inner or outer angle, and its size and shape are critical parameters for wing performance. Winglets can increase the range and reduce fuel consumption. With split winglets, the expected reduction in fuel consumption is up to 1.5 %. This type of additional surface on the wing increases the effective aspect ratio of the wing without increasing the structural load. This paper investigates the performance of the wing with and without the split winglets and constant airfoil b737c-il at angles of attack (0° , 10° and 20°), at the speed of 0.8 Mach. Wing model was designed in CATIA P3 V5 software package. The aerodynamic drag and lift coefficients C_D and C_L , as well as their change with the angle of attack, were obtained by finite volume method (FVM) in ANSYS Fluent software.

Keywords: Winglets, aerodynamic coefficients, performance of the wing, CFD.

1. INTRODUCTION

The initial design of winglets dates back to 1897. English engineer Frederick W. Lanchester patented wing end-plates as a method for controlling wingtip vortices. In the USA in 1910, Scottish engineer William E. Somerville patented first functional winglets, when he used them for his design of monoplane. The term winglet was previously used to describe an additional lift surface on the plane, such as a short part between wheels on a fixed landing gear. The research of Richard Whitcomb in 1970. at NASA is the first research in which a winglet was used with its modern meaning, which relates to the vertical extension of the wing. In 1990. McDonnell Douglas MD-11 was the first plane with the split winglets. Nowadays the Boeing 737 MAX, is using a new version of this type of winglet, which consist of a two-sided hybrid. This is the latest design that should enable additional 1.5% savings in fuel with respect to the already projected 10–12% on this plane [1].

This paper provides a comparative analysis of aerodynamic performances of wings with and without

split winglets at three different angles-of-attack (AoA), 0° , 10° and 20° , and cruising speed of 0.8 Mach. Both wings have constant airfoil b737c-il along the span.

Results will be quantified through the aerodynamic coefficients C_D and C_L , as well as representation of their change with the angle of attack and pressure which appears on the wing in the moments when we have speed of 0.8 Mach and different angles of attack [2]. The representations of wing and winglet models are given in Fig. 1 and Fig. 2, respectively.

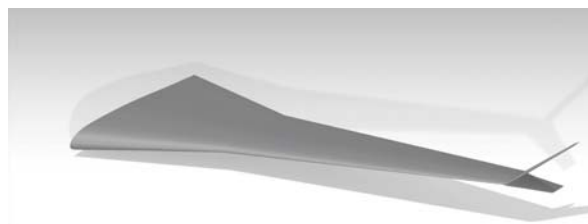


Figure 1. Model of wing

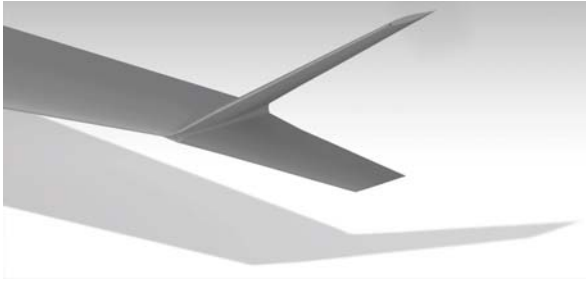


Figure 2. Model of winglets

2. MODEL DESCRIPTION

Airfoil which presents the cross-section of this wing is b737c-il with maximum thickness 10% at 39.9% chord and maximum lift coefficient around $C_{L,max} \approx 1.0$. Airfoil is illustrated in Fig. 3.

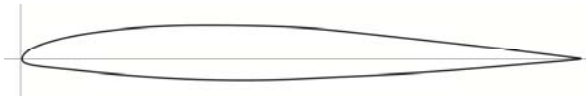


Figure 3. Airfoil b737c-il

In reality, the b737c-il is a midspan airfoil used at the initial Boeing 737 MAX wing only at a length of 6 m. B737a-il is used at the root and b737d-il at the end of the wing, and they have different relative thicknesses. In this study, for simplicity reasons, a constant airfoil is assumed along the span of the wing. It can be considered that this airfoil is of sufficient quality to adequately represent the wing in real flight conditions.

2.1. Geometry

Model of wing is realized in software CATIA, in module Generative Shape Design. Geometric parameters of the wing are given in Table 1, and their illustration in Fig. 4.

Table 1. Parameters of wing

Parameters	Values
Wing half-span with winglets	18.45 [m]
Wing half-span without winglets	16.837 [m]
Mean aerodynamic chord of wing	4.41 [m]
Mean aerodynamic chord of winglets	1.03 [m]
Wetted wing area with winglets	133.4 [m ²]
Wetted wing area without winglets	124.0 [m ²]
Dihedral of wing	5.15°
Inner angle of winglets	100°
Outer angle of winglets (upper surface)	141.15°
Outer angle of winglets (lower surface)	118.85°

Parameters of the wing imitate the initial Boeing 737 MAX wing that is illustrated in Fig. 4. Assumed take-off mass is $m_{TOW} = 80$ t.

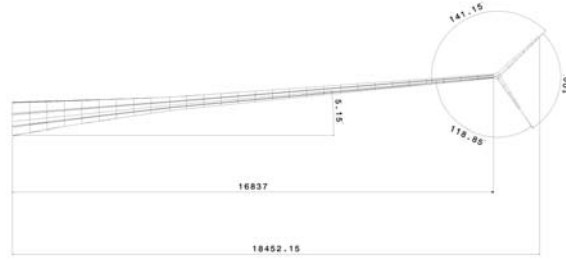


Figure 4. Illustration of wing and winglet parameters

3. ASSESSMENT OF AERODYNAMIC LOADS

The purpose of this paper is to compute aerodynamic loads and coefficients, when Mach number is 0.8 and angles of attack are 0°, 10° and 20°. Results are also presented by the pressure (and pressure coefficient) and Mach number distributions as well as vorticity iso-surfaces that were calculated in software ANSYS Fluent.

3.1. Lift and drag

The generation of lift force on wings happens because of the pressure imbalance between the bottom surface that is high pressure and the top of surface that is low pressure. In the case of finite-span wings, higher pressure air flows around the edges and tries to displace the lower pressure air on the top of the wing. These phenomena are called wingtip vortices and can be associated with high velocities and low pressure. Winglets are designed to decrease the negative effects of tip vortices. These vortices affect velocity and produce local relative downward wind, which reduces angle of attack of the wing. As a result, additional force components are generated. That is a component of drag, which is a sum of parasite drag and induced drag. Parasite drag is also known as the drag coefficient at zero lift and is independent of the lift. Equation (1) represents total drag of the wing:

$$C_D = C_{D0} + C_{Dind} \quad (1)$$

Lift-induced drag coefficient C_{Dind} is defined in Equation (2) like ratio of squared C_L - the wing lift coefficient, λ - wing aspect ratio and e - Oswald efficiency factor or wingspan efficiency [3].

$$C_{Dind} = \frac{C_L^2}{\pi \lambda e} \quad (2)$$

3.2. Numerical methods

Flow analysis is done in ANSYS FLUENT, by numerically solving the equations that govern the air flow. ANSYS FLUENT uses a finite volume approach to calculate the flow variables [4]. The Shear Stress Transport (SST) $k-\omega$ model has been chosen to model the effects of turbulence. The flow is assumed to be

spatial, stationary, compressible and viscous. This turbulence model is considered with air as ideal gas as the material. In this method k is the turbulent kinetic energy and ω is specific dissipation rate, which is presented in Equations (3) and (4):

$$\frac{\partial k}{\partial t} + (u - \sigma_k \nabla v_t) \nabla k - \frac{1}{P_k} \nabla^2 k + s_k = 0 \quad (3)$$

$$\frac{\partial \omega}{\partial t} + (u - \sigma_\omega \nabla v_t) \nabla \omega - \frac{1}{P_\omega} \nabla^2 \omega + s_\omega = 0 \quad (4)$$

In these equations the turbulent viscosity and effective Peclet numbers are defined as:

$$v_t = \frac{k}{\omega} \quad (5)$$

$$P_k = \frac{1}{\frac{1}{R_e} + \sigma_k v_t} \quad (6)$$

$$P_\omega = \frac{1}{\frac{1}{R_e} + \sigma_\omega v_t} \quad (7)$$

The Shear Stress Transport (SST) $k-\omega$ model requires refinement near the walls, i.e. that dimensionless wall distance satisfies $y^+ \leq 1$ [5].

Along the outer boundaries assumed turbulence intensity is 0.05%, and turbulent viscosity ratio is 10.

$$\begin{aligned} v_t / \nu &= 10, \\ k &= 0.0161 \frac{\text{m}^2}{\text{s}^2}, \\ \omega &= 57.23 \frac{1}{\text{s}}. \end{aligned} \quad (8)$$

3.3. CFD analysis

This analysis with $k-\omega$ SST turbulence model is specifically designed for aerospace applications involving wall-bounded flows and in this paper it has been shown to give good results for boundary layers subjected to adverse pressure gradients.

Value of operating pressure and temperature is on sea level condition and for all the walls the adiabatic, no-slip boundary conditions are used. Based on density $\rho = 1.225 \text{ kg/m}^3$, cruising velocity $V_{cr} = 0.8 \cdot 340 \text{ m/s} = 272 \text{ m/s}$, mean aerodynamic chord $l_{SAT} = 4.41 \text{ m}$ and viscosity $\mu = 1.789 \cdot 10^{-5} \text{ kg/ms}$, Reynolds number is $\text{Re} = 6.64 \cdot 10^7$ [5]. Assumed Mach number of $M = 0.8$ corresponds to cruising flight condition. Critical Mach number that changes with the angle of attack is somewhat smaller. With these parameters and assumed take-off mass, the value of lift coefficient at cruise is approximately $C_{L,cr} = 0.13$. Velocity components are computed from velocity magnitude and angles-of-attack, and obtained results are presented in continuation.

For this analysis meshing process is done in ANSYS Meshing, with unstructured tetrahedral elements. Characteristics of the mesh are listed in Table 2.

To better simulate the effect of wing walls in fluid flow, 15 layers of thin cells encompass the wall surfaces.

Table 2. Mesh details

Mesh Details	Values
Number of Nodes	1414953
Number of Elements	4166070
Number of Layers	15

As previously mentioned, the geometric model is spatial. Computational domain, representing the fluid around the wing, is shaped like a cuboid. It extends 95 m fore of the wing, and 160 m aft of the wing along the x -axis, as illustrated in Fig. 5. Figure 6 provides a detail of the mesh around the wing.

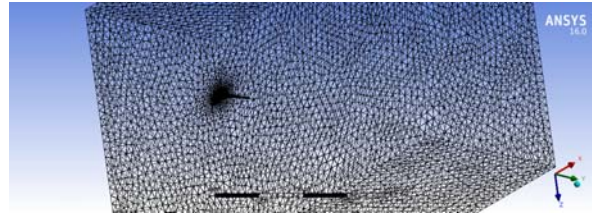


Figure 5. Computational mesh of fluid domain

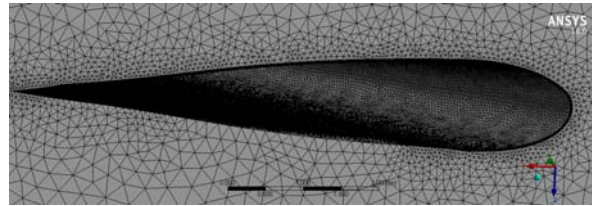


Figure 6. Detail of the mesh around the wing

This is a preliminary study conducted on a medium-fine mesh because the calculations are quite demanding. Viscous, compressible fluid was considered. In some of the following studies, the finer mesh will be considered, for more accurate results.

4. RESULTS AND DISCUSSION

The outcomes of the performed study are presented by comparing the results of wing with winglets and wing without winglets. That is important for discussion about the influence of winglets to reduce drag and increase lift coefficients. CFD analysis for wing without winglets is done with the same numerical setting like analysis for wing with winglets and for the same flight conditions. The representation of the pressure field is important to show that the pressure is higher in the zones of stall speed, while lower values appear at the points of separation of the air flow. Determining the pressure field is also very important for structural design and definition of load carrying elements and as an input for structural

analysis. Comparing these results with the flight tests, would lead to the final decision of the conceptual design.

For this study, we can say that this is a simulation of flight conditions in a wind tunnel with density at sea-level. Computed values of aerodynamic coefficients for wing with and without winglets are presented in Table 3 and Table 4, respectively. Results obtained at different angles of attack are listed. Cruising flight case corresponds to zero angle of attack.

Table 3. Aerodynamic coefficients of wing with winglets

Wing with winglets			
α	C_L	C_D	C_L/C_D
0°	0.1597	0.0193	8.2664
10°	0.7517	0.1648	4.5615
20°	0.9294	0.3714	2.5024

Table 4. Aerodynamic coefficients of wing without winglets

Wing with winglets			
α	C_L	C_D	C_L/C_D
0°	0.1611	0.0197	8.1827
10°	0.7306	0.1664	4.3909
20°	0.9070	0.3689	2.4586

By analyzing results of aerodynamic coefficients in this preliminary study, the influence of winglets can be observed on aerodynamic performance of wing. Both lift and drag coefficients are slightly higher for wing with winglets, as a consequence of added surfaces. However, beneficial effects on lift are higher, resulting in slightly increased lift-to-drag ratio and improved polar as illustrated in Fig. 7.

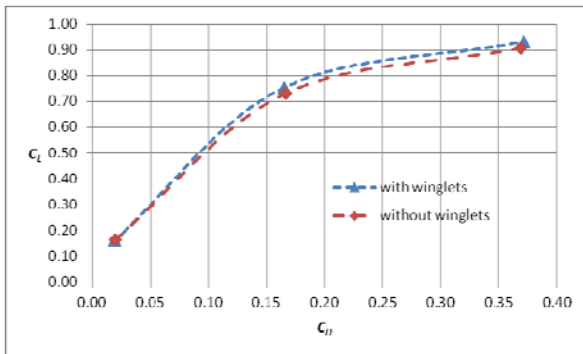


Figure 7. Computed polars

If the same values of range $R = 7000$ km and specific fuel consumption $c = 0.5 \text{ h}^{-1} = 14.1 \text{ mg/Ns}$ are assumed for both wings, for given cruising speed V_{cr} and computed lift-to-drag ratios it is possible to estimate and compare the ratios of masses (and weights) before and after the cruising segment that point to the spent fuel according to:

$$R = \frac{V_{cr}}{c} \frac{L}{D} \ln \frac{W_{init}}{W_{end}} \tag{9}$$

Slightly improved lift-to-drag ratio of the wing with winglets implies that it is possible to save up to 1% of fuel. This value could further be increased by more detailed study and simulations.

Pressure field computed along the wing surface, at zero AoA, is illustrated in Fig. 8, where the maximum obtained value is $1.482 \cdot 10^5$ Pa. The extents of the sonic bubble appearing on the upper surface are clearly visible.

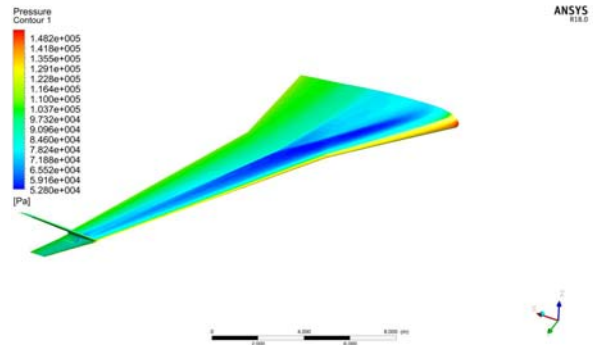


Figure 8. Field of pressure, angle of attack 0°

At angle of attack of 10° maximum value of pressure is $1.479 \cdot 10^5$ Pa. This value is slightly lower than in the previous case, but a change in the fluid flow is clearly seen in Fig. 9.

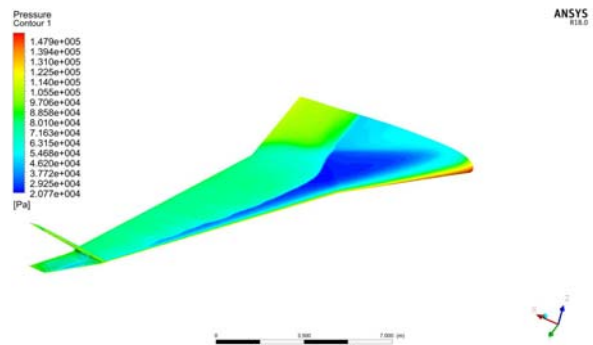


Figure 9. Field of pressure, angle of attack 10°

It is also possible to compare the local pressure coefficient distributions. Two cross-sections are chosen: $y_1 = 10$ m and $y_2 = 15$ m. The first one is located approximately at 2/3 of the half-span and the second in the vicinity of wing tips. Distributions presented in Fig. 10 at angle of attack $\alpha = 10^\circ$ demonstrate that the effect of winglets stretch towards the wing root and are not only present near the wing tips. They are particularly visible near the leading upper surface.

Figure 11 illustrates the extents of the sonic bubbles appearing along the suction surfaces of wings with and without the winglets while cruising at zero angle of attack.

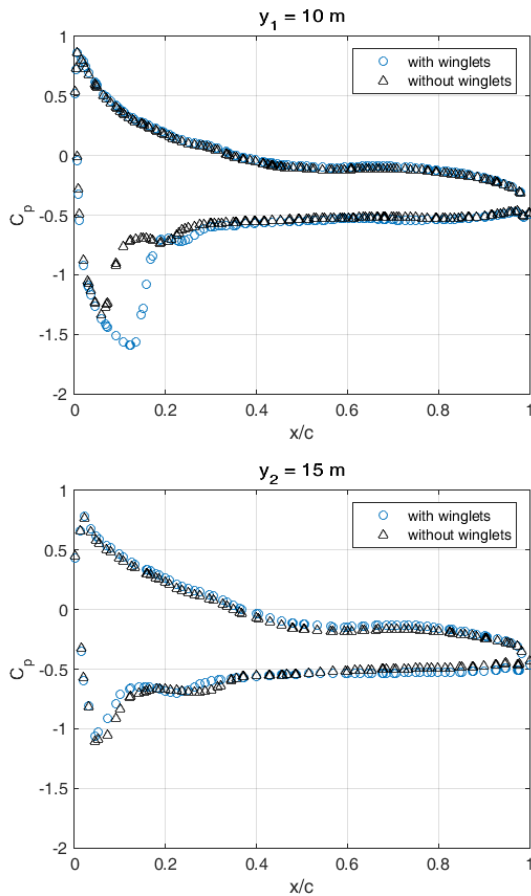


Figure 10. Pressure coefficient distributions at angle of attack 10°



Figure 11. Sonic bubbles at angle of attack 0°

Again, as with pressure coefficient distributions in Fig. 10, it can be observed that the presence of winglets somewhat changes the velocity distribution around the complete half-wing and not just near the wing tips.

Finally, Fig. 12 illustrates the vortices detaching from both investigated wings as well as zones of highest vorticity at zero angle of attack.

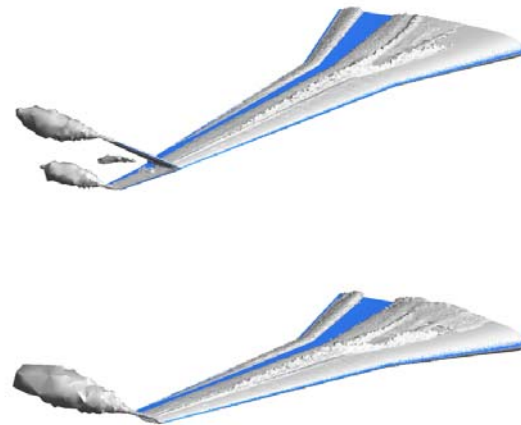


Figure 12. High vorticity zones at angle of attack 0°

It can be observed that specially designed wing tips can significantly affect the shape and reduce the intensity of tip vortices.

5. CONCLUSION

The aim of this paper was the computational analysis of the wing with split winglets, and estimation of its aerodynamic performances at different angles of attack in comparison to the same wing without winglets. Although a preliminary study was performed, the presented numerical and graphical results indicate that split winglets can positively alter the flow field around the wing.

Design modification in wing construction, by adding winglets to reduce the drag and tip vortices and increase lift, is one of the possible ways to increase aircraft efficiency and reduce fuel consumption. To better quantify the positive effects of split winglets, more detailed numerical studies will be performed.

References

- [1] Shamil PC., Mohammed S., Muhammed E., Aravind K., Prof. Thomas J., *Performance analysis of winglet using CFD*, International Research Journal of Engineering and Technology, vol. 05, issue:04 April, 2018.
- [2] Hesham S.M.H., Essam E.K., Osama E.A., Gamal M.E., *Aerodynamic Analyses of Aircraft-Blended Winglet Performance*, Journal of Mechanical and Civil Engineering vol. 13, issue:3, ver. IV May-Jun, 2016.
- [3] Gavrilovic N., Rasuo B., Dulikravich G., Parezanovic V., *Commercial aircraft performance improvement using winglets*, FME Transactions, vol.43, No 1, 2015.
- [4] Zabihollah N.A., Ahmed S., *Improving the aerodynamics performance of a wing with winglet*, International Journal of Natural and Engineering Science, November 2014.

- [5] Svorcan J., Baltic M., Ivanov T., Pekovic O., Milic M., *Numerical evaluation of aerodynamic loads and performances of vertical-axis wind turbine rotor*, International Congress of Serbian Society of Mechanics, Sremski Karlovci, Serbia, June 24-26, 2019.